Hindawi
Shock and Vibration
Volume 2017, Article ID 3252543, 18 pages
https://doi.org/10.1155/2017/3252543

Research Article

Investigation of Axial Strengthened Reinforced Concrete Columns under Lateral Blast Loading

Mohammad Esmaeilnia Omran and Somayeh Mollaei

Department of Civil Engineering, University of Kurdistan, Sanandaj, Iran

Correspondence should be addressed to Somayeh Mollaei; s.mollaei@eng.uok.ac.ir

Received 26 May 2017; Revised 25 August 2017; Accepted 6 September 2017; Published 16 October 2017

Academic Editor: Abdul Qadir Bhatti

Different factors can affect blast response of structural components. Hence, experimental tests could be the best method for evaluating structures under blast loading. Therefore, an experimental explosion loading has been done on RC members by the authors. Four RC components, with identical geometry and material, with and without axial load were imposed to air blast. Observed data of the members' response under blast loading was used for validation of finite element modeling process using ABAQUS software. With respect to complexity, limitations, and high costs of experimental tests, analytical studies and software modeling can be good alternatives. Accordingly, in this paper, the behavior of 6 different models of normal and strengthened RC columns under blast loading was evaluated using ABAQUS. Strengthening configurations considered here were designed for enhancing axial capacity of RC columns. Therefore, we can investigate the effectiveness of axial strengthening of column on its blast resistance capacity and residual axial strength. The considered strengthening methods were different steel jacket configurations including steel angle, channel, and plate sections. The results showed that retrofitting significantly improves blast performance of the columns. Moreover, residual strength capacity of the columns strengthened with steel channel is higher than the other models.

1. Introduction

A wide range of engineering structures such as high-rise buildings, bridges, tunnels, dams, platforms, and military and security shelters are constructed by reinforced concrete materials. There has been much attention to reinforced concrete (RC) structures performance under static and seismic loads but evaluation of RC structures' behavior under blast loading and identification of their dynamic characteristics are important for valid design of concrete structures given that many structures may face extreme dynamic loading such as explosion in their lifetime. Columns are the key load bearing elements in building structures and in case of an explosion event near the building, columns are mostly the first structural elements which are affected by lateral loading caused by explosion. Studying the explosion of explosives has been considered by scientists and researchers and the efforts of scientists and researchers in the field of shock wave physics became important since the 20th century [1]. One of the pioneers in this field is Hopkinson (1915) who conducted extensive research and tests and formed the Hopkinson-Cranz scaling law [1, 2].

Recently, many different studies have been conducted on different types of concrete structures such as columns under explosion loads [3–7]. With respect to complexity, limitations, and high cost of laboratory researches in this field, analytical studies and software modeling can be a good alternative to laboratory and experimental methods. Finite element analysis method is a powerful and useful tool for researchers and structural designers to have an accurate estimation of behavior of structures under blast loading without requiring high costs and great difficulty. Shi et al. (2008) defined a failure criterion based on residual axial capacity for reinforced concrete columns and drew *P-I* (pressure-impulse) diagrams for columns based on this failure criterion using numerical modeling by LS-DYNA software [8]. Bao and Li (2010) conducted parametric studies on RC columns using numerical modeling in LS-DYNA [3]. In line with the most important results, reinforced concrete columns must be designed in such a way that their moment

capacity should be less than shear capacity. On the other hand, lateral deformation of column must be controlled in order to prevent instability caused by secondary moments. In this study, standoff distance has been considered to be constant and explosion has been considered to occur at a close distance. A similar study has been carried out by Wu et al. (2011) using arbitrary Euler–Lagrange analysis in LS-DYNA software for analysis of columns' response under contact explosion [9]. The results obtained have been used for evaluation of residual axial capacity of columns and the effect of different parameters on this capacity has been evaluated. ABAQUS/Explicit software has been used in finite element modeling by Arlery et al. (2013) on effects of close explosion on reinforced concrete columns [10]. In line with the results, depth of column section and distance to the center of the explosion had the greatest effects in reducing the amount of damage in the column and height and width of section and concrete compressive strength are less effective [10]. Center of the explosion is extremely close to the structure in this study and the response of structure in this case is usually local and in form of erosion of section. A numerical study was carried out by Kyei and Braimah (2017) to investigate the effects of transverse reinforcement spacing on the blast resistance of RC columns using LS-DYNA code. The study revealed that the effect of transverse reinforcement spacing and axial loading significantly affects RC column behavior under blast loading at low scaled distances. At higher scaled distances, however, the effects were insignificant [11].

Some researchers have studied the retrofitting and strengthening of RC columns under the blast loading. Crawford (2013) reported some of the methods of using FRP for strengthening RC columns in order to increase the strength of RC columns under the simultaneous effect of blast loading and axial force [6]. According to the main results, FRP coating increases the ductility and shear strength of the column. The focus in these studies was based on FRP material and other methods for retrofitting RC columns were not considered. Carriere et al. (2009) have introduced SRP covers as a perfect replacement for CFRP for retrofitting RC elements against explosion [12]. The effect of retrofitting reinforced concrete beams and columns using SRP coating has been evaluated using explosion tests and numerical modeling by AUTODYN. Based on the obtained results, SRP coatings have lower cost and easier installation process in comparison to CFRP covers. Also, SRP increases ductility of RC columns under blast loading and prevents brittle collapse of RC columns. Nevertheless, there has been no reference to displacements or strains in the considered samples and also the scales of studied samples are small. Xu et al. (2016) discussed the blast resistance of UHPC (ultra-high performance concrete) columns by conducting a series of field tests. It was reported that UHPC materials provide sufficient strength, ductility, and energy absorption and crack controlling capacities compared to conventional normal strength concrete [13]. Zhang et al. (2016) reported an experimental investigation on Concrete-filled double-skin tubes (CFDST) columns subjected to blast loading. Based on the results, it was obvious that CFDST column has excellent blast resistance and it can prevent concrete crushing and steel buckling and thus has an overall global flexural response as opposed to localized structural failure [14].

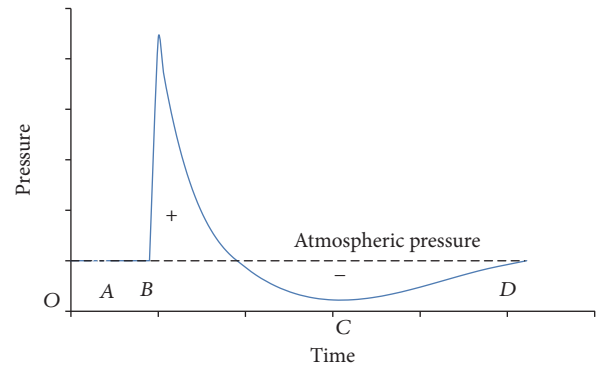

Figure 1: Pressure-time diagram of blast wave.

By reviewing literature, it can be observed that retrofitting effects have been considered in minor studies. Moreover, most studies about blast retrofitting of RC columns have been considered using polymer sheets. On the other hand, the need for further studies in this field still remains due to uncertainties in the phenomenon of explosion and complexity of the behavior of RC sections under lateral blast loading. Thus, in this paper, 6 models of retrofitted RC columns have been evaluated under blast loading. The effects of different configuration of steel jackets have been investigated using ABAQUS 6.13 software [15]. All of the strengthening configurations considered here were designed with the purpose of enhancing the axial load bearing capacity of the RC columns. Therefore, we can investigate the effectiveness of axial strengthening of the RC columns by steel jackets on their blast resistance capacity.

2. Blast Loading

Explosion is an instantaneous phenomenon which creates large amounts of light, heat, sound, and pressure resulting from blast wave due to sudden release of large amounts of energy. The real source of this energy can be gunpowder, steam compressed in the boiler, or uncontrolled nuclear developments. However, release of energy should be sudden and a high-energy environment should be formed around it. A part of this energy is released through heat radiations and a part of it enters into the air (air blast) and ground (ground shock) through radial waves [18]. An approximate pressure-time diagram at a certain distance from the center of the explosion is drawn in Figure 1. As can be seen in the figure, Section A corresponds to time before the arrival of the wave front and B is after incident shock impact and shows the sudden increase of pressure. Positive pressure has ended at C and negative phase of pressure (suction) can be felt in the environment. This is alongside the blast wind in the opposite direction to the direction of incident shock impact and D corresponds to the disappearance of blast wave effects and return of pressure to atmospheric pressure [19].

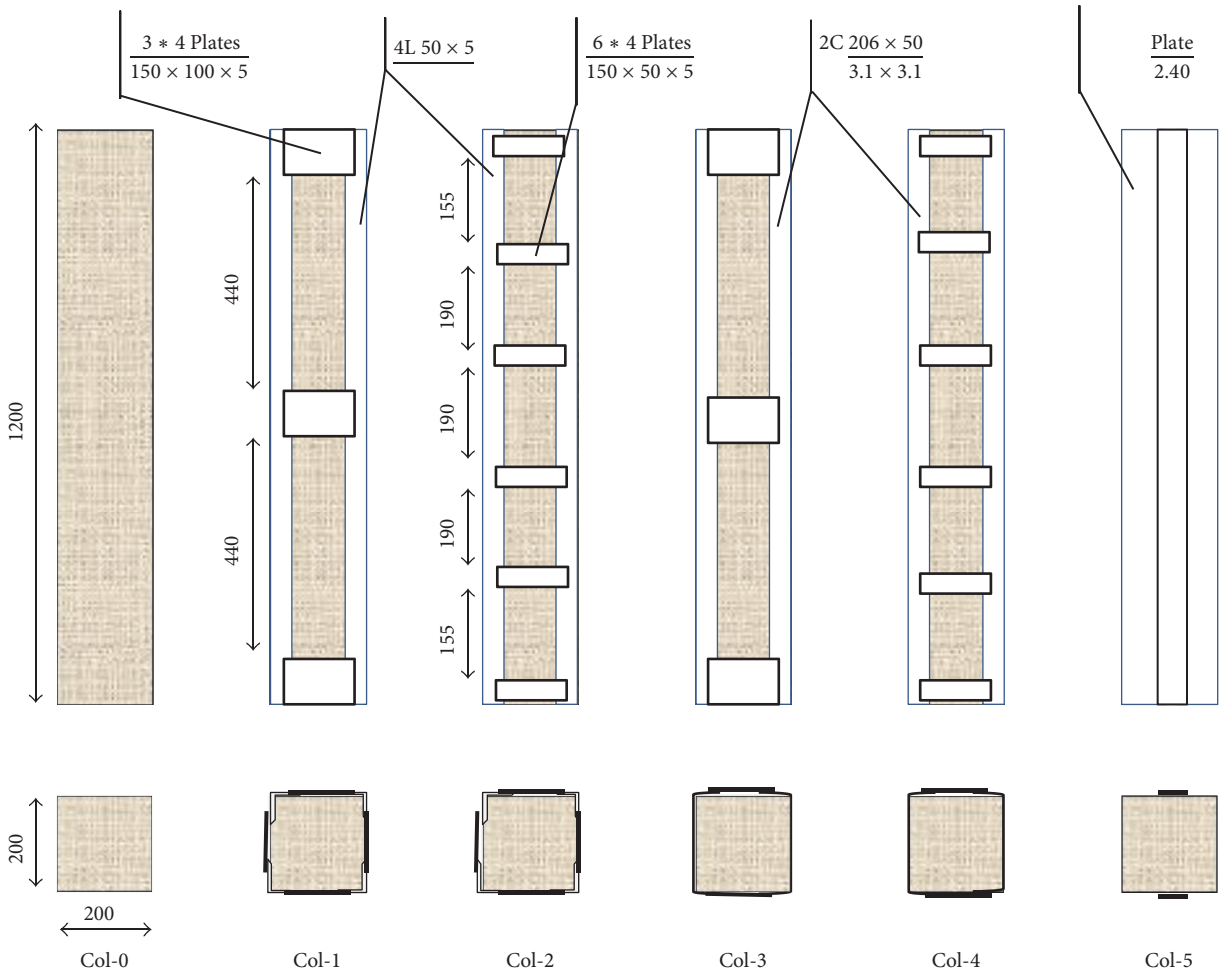

Figure 2: Details of dimensions and retrofitting configuration of columns [16].

Methods for estimation of pressure diagram for an explosion and its distribution on structural face have been presented in many different references [18–21].

3. Details of the Studied Models

Here, RC columns with the specifications provided in [16] by Belal et al. (2015) have been used. Six models of RC columns were considered; one of them is simple (not retrofitted) while others are retrofitted using different configuration of steel jackets. Characteristics of the section and details of retrofitting methods for all samples are summarized in Figure 2 and Table 1. Columns have rectangular symmetric section with dimensions of 200 mm and height of 1200 mm which retrofitting offered in order to increase their axial bearing capacity. Steel elements used in strengthening of samples have been used in such a way that they all have equal horizontal cross-sectional area [16].

Concrete compressive strength used in samples is 34 MPa which is the same for all samples. Specifications of steel materials have been mentioned in Table 2 and failure strain here is the strain which corresponds to ultimate tensile stress of steel material.

4. Finite Element Modeling

Here, finite element models of columns and steel jackets have been initially developed and then these models have been analyzed under lateral blast loading. Proper modeling and meshing of reinforced concrete and steel as well as the interaction between them are important factors in development of accurate models. Details of modeling process are explained in this section.

4.1. Modeling of Concrete Material. Concrete damage plasticity (CDP) model has been used in this study for modeling of concrete's behavior which was presented by Lubliner et al. (1989) [22] and was later completed by other researchers [23, 24]. Two main failure mechanisms including tensile cracking and compressive crushing are assumed for concrete in this model. Nonlinear behavior of concrete is described using isotropic damage elasticity and tensile and compressive plastic concepts. Figure 3 shows stress-strain curves for concrete material in uniaxial tension and compression.

In Figure 3, E_0 is the modulus of elasticity, σ_t is tensile stress, σ_c is compressive stress, $\tilde{\varepsilon}_t^{ck}$ is cracking strain, $\tilde{\varepsilon}_t^{in}$ is inelastic strain associated with existing stress, and d_t

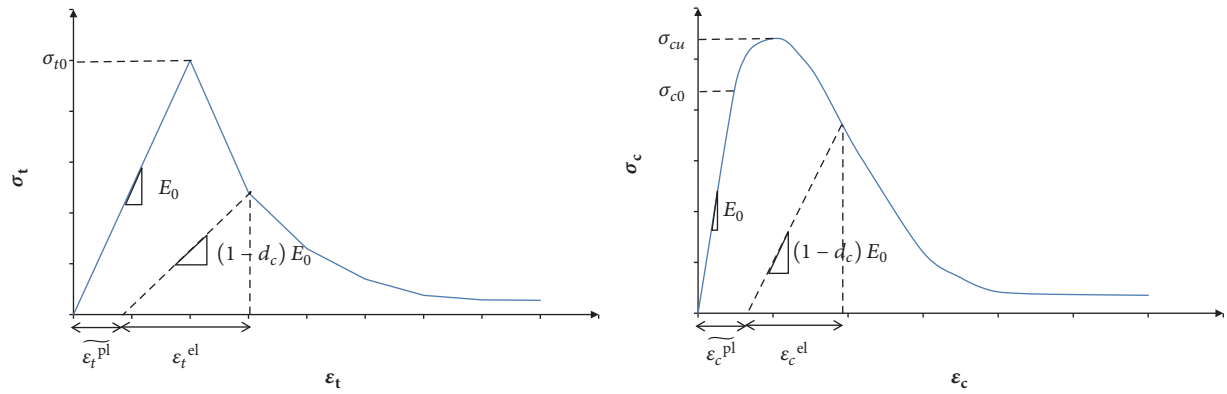

(a) (b)

Figure 3: Uniaxial behavior of concrete; (a) tension; (b) compression [15].

Table 1: Specifications of models (dimensions: mm).

Model	Strengthening configuration	Longitudinal and transverse reinforcement	Dimensions
Col-0	Without strengthening	4 ϕ 12 - ϕ 8 @ 100	200 × 200 × 1200
Col-1	Steel angles 4 L 50 × 50 × 5 + 3 × 4 plates 150 × 100 × 2	4 ϕ 12 - ϕ 8 @ 100	200 × 200 × 1200
Col-2	Steel angles 4 L 50 × 50 × 5 + 3 × 4 plates 150 × 50 × 2	4 ϕ 12 - ϕ 8 @ 100	200 × 200 × 1200
Col-3	Steel channels 2C (206 × 50)/(3.1 × 3.1) + 3 × 4 plates 150 × 100 × 2	4 ϕ 12 - ϕ 8 @ 100	200 × 200 × 1200
Col-4	Steel channels 2C (206 × 50)/(3.1 × 3.1) + 3 × 4 plates 150 × 50 × 2	4 ϕ 12 - ϕ 8 @ 100	200 × 200 × 1200
Col-5	Complete steel jacket (steel plates) 4 × 4 plates 200 × 2.4	4 ϕ 12 - ϕ 8 @ 100	200 × 200 × 1200

Table 2: Specifications of steel material.

Material	Nominal diameter (mm)	Modulus of elasticity (MPa)	Yield strength (MPa)	Ultimate stress (MPa)	Failure strain
Longitudinal bars	12	210000	360	463	11
Stirrups	8	210000	240	340	14

and d_c are damage parameters in tension and compression, respectively. Completion of failure surface is controlled using hardening variables of ε_c^{pl} and ε_t^{pl} which are, respectively, related to failure mechanisms under compressive and tensile loading [15]. In fact, ε_c^{pl} and ε_t^{pl} are equivalent plastic strains. Stress-strain curve changes linearly until the failure stress point σ_{t0} due to uniaxial tensile of stress-strain curve and these stresses are along with onset and extension of small cracks in concrete. Damage will be visible in form of cracks after passing the mentioned point which is shown in form of softening regime in stress-strain space. Response in uniaxial compressive will be elastic until reaching σ_{co} yielding point and behavior in plastic zone is generally expressed in form of hardening regime and curves will change to softening curves in the end by reaching the point of ultimate tension σ_{cu} [15].

4.1.1. Failure Criterion. William-Warnke failure criterion and Hillborg failure energy model (1976) are used to describe the failure and crack propagation in CDP model. The general form of William-Warnke failure criterion is in the form of

$$F(I_1, I_2, I_3) = 0, \tag{1}$$

where I_1, I_2, and I_3 are the first, second, and third stress tensor invariables, respectively. This failure surface is a cone-like shape in the stress space. Each form of stress corresponds to one point in stress space. If this point is out of space defined in the above equation, it shows the failure of material [15]. The brittle behavior of concrete in Hillborg failure energy model is more determined by stress-displacement response than by stress-strain response under the tension. Crack failure energy model can be achieved using the expression of tensions after failure as a function of crack's width [15].

In the CDP model used here, values for dilation angle, eccentricity, f_{b0}/f_{c0} ratio (compression biaxial yield stress to uniaxial yield stress), k yield level parameter, and viscosity parameter (μ) have been considered to be equal to 40, 0.1, 1.16, 0.6667, and 0.001, respectively.

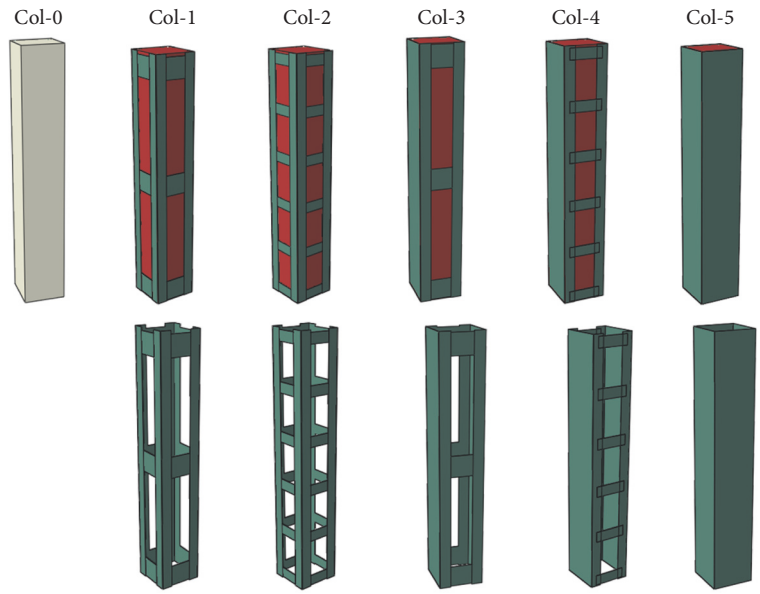

Figure 4: Finite element models of studied RC columns.

4.2. Modeling of Steel Material. In this study, steel reinforcing bars have been modeled separately and with dimensions similar to those used in real samples. Steel material behavior has been assumed to be linear elastic-perfectly plastic. It should be noted that the behavior of steel has been considered to be isotropic. In all stages, Von-Mises surface model is used here for steel. In this model, yielding has been considered to be isotropic and it has been assumed to be a function of main stresses and when deviatoric stress reaches a critical value in the main stresses space, yielding occurs. This model is defined in the form of the following equation:

$$\Phi = \frac{1}{2}\left[(\sigma_1 - \sigma_3)^2 + (\sigma_1 - \sigma_2)^2 + (\sigma_2 - \sigma_3)^2\right] - {F_y}^2. \quad (2)$$

In this equation, σ_1, σ_2, and σ_3 describe the main stresses and F_y is the yield stress of material. In fact, the above equation describes a three-dimensional space in which each mode of stress corresponds to one point in the stress space. If this point is out of three-dimensional cylinder defined by the above equation, it shows the yielding of material. At this model, effect of hardening is not considered [15].

4.3. Concrete and Reinforcement Interaction. The interaction between concrete and steel reinforcing bars is a very important parameter in modeling of RC structures. This interaction as a factor causes continuity between steel and concrete materials and thus makes it possible to use the whole capacity of materials including concrete compressive strength and tensile strength of steel bars. Embedded element model has been used in this study for modeling of interaction between concrete and steel elements. In this technique, if a node of steel elements is placed in concrete elements, degrees of freedom for that node are removed and node becomes a buried node. Thus, the degrees of freedom for buried node are calculated using the degrees of freedom of concrete elements adjacent to this node. Therefore, degrees of freedom of each buried node depend on degree of freedom of concrete element node adjacent to it [15].

4.4. Meshing and Elements. C3D8R solid element has been used for three-dimensional modeling of concrete. This element is a three-dimensional cube with 8 nodes which uses reduced integration method. T3D2 truss element has been used for modeling of steel bars which is a three-dimensional truss element with 2 nodes. This element has been selected because axial force plays a key role in the analysis of bars and there is no need for elements with several nodes. Thus, volume and time of computation will be significantly reduced. S4R shell element has also been used for modeling of steel jacket which is three-dimensional shell element with 4 nodes and 6 degrees of freedom [15].

Figure 4 shows finite element models of RC columns with different types of steel jacket retrofitting configuration. In the next section, these columns will be evaluated under the effect of blast loading.

4.5. Loading and Boundary Conditions. Blast loading applied on columns has been done based on the methodology proposed in UFC 3-340-02 [19]. Determined pressure has been applied to lateral surface of the column. Figure 5 shows pressure-time curve and applied pressure for blast loading of the retrofitted columns model.

5. Experimental Program

In the present study, a field test was conducted to investigate the behavior of conventional columns subjected to blast loading. In total, four 0.35 m × 0.35 m RC members with the same reinforcement and span length of 3 m were tested under an explosion loading at a standoff distance of 3 m. Blast test was performed on two reinforced concrete columns with initial axial force and two columns without

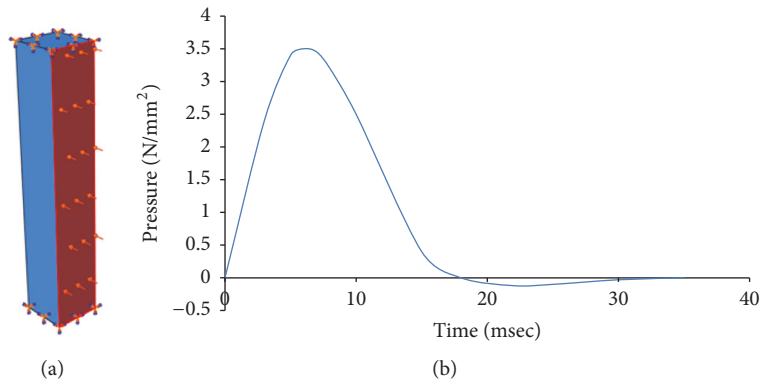

Figure 5: Blast pressure-time history (b) and applied blast load (a).

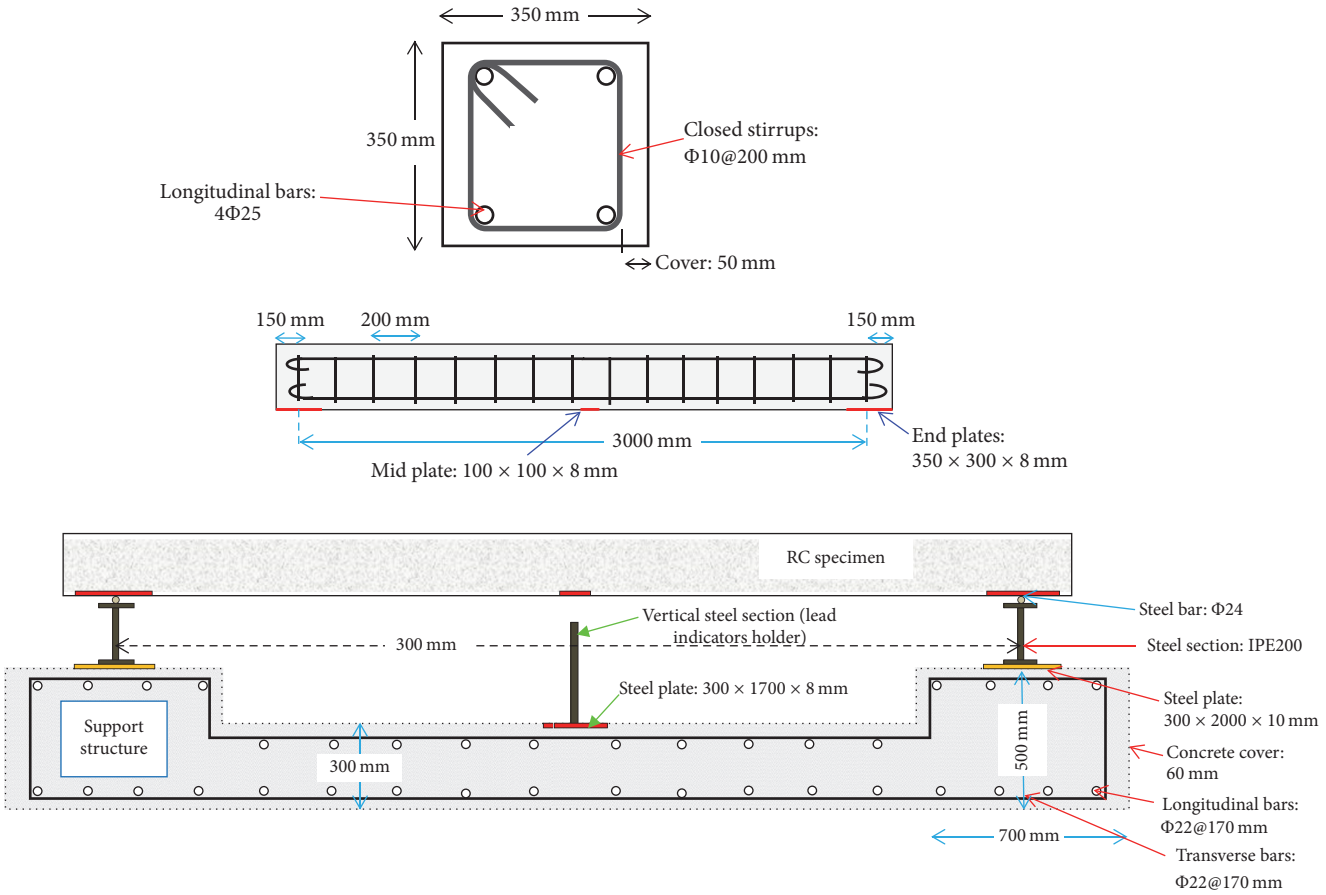

Figure 6: Cross section and reinforcement details of the specimen and support condition.

axial force to evaluate their behavior under the same loading conditions. RC components not forming part of the seismic force resisting system were detailed according to ACI 318-14 [25]. The data collected from each specimen included maximum transverse displacement (deflections at center), axial strain of longitudinal bars, and postblast crack patterns. Recorded data from this test were used in order to validate FEM modeling and analysis process. Charge weight including 20 kg of cartridge emulsion explosive with density of 1.165 g/cm^3 and velocity of detonation of 5800 m/s (27 mm diameter) is used such that TNT equivalent factor is about 0.90 (W = 18 kg-TNT). Dimensions and reinforcement details of the samples are shown in Figure 6. All the samples were placed horizontally simply on the support structure so that there were pinned support conditions at both ends of the samples. Characteristic compressive strength of the concrete, used for construction of the samples, was determined by laboratory tests and its average value was

(a)

(b)

Figure 7: Test setup for blast loading of the specimen (a) and aerial photos of the explosion event (b).

30 MPa. AIII steel bars with yield strength of 400 MPa and ultimate strength of 600 MPa were used as longitudinal and transverse reinforcement as well as posttensioning system.

In order to impose constant axial compressive load on the samples, 6 posttensioned steel bars were used and each bar had been initially tensioned using click-type torque wrench (Britool Expert HVT7200 (200–810 N·m)). In each case, the bars were anchored to a 50 mm thick steel plate at two ends of the columns. Constant axial stress in each steel bar was 100 kN and there were six posttensioning bars in every column. Hence, there is an axial force of 600 kN in two posttensioned columns (equal to 16% of the static axial load capacity of the column). In Figure 7, the test setup and aerial photos of the explosion event are shown.

Axial strain gauges (FLA-3-350-11, 350 Ω (Tokyo Sokki Kenkyujo Co. Ltd.)) were installed on the longitudinal bars at half-length of the samples. The data transferred from strain gauges during the blast loading are recorded using digital data acquisition card DAQ- NI USB-6009 (National Instruments Corporation). Lead rods were installed under the samples as maximum displacement indicators at mid length. There were two lead rods under each sample and comparing their length before and after blast loading could show the maximum displacement of the column at mid length. Figure 8 shows the shape of the indicator rods before and after blast loading. Based on the results, average amount of lateral displacement of the columns with and without axial load under blast loading is 3.5 and 8 mm, respectively.

FE modeling and analysis of the columns were done using the process described in Section 4. For imposing axial load, a rigid part was modeled at one end of the column. Deformed shape and main crack pattern of the column models under blast loading are shown in Figure 9. Maximum transverse displacement of a nod at mid length of the models with and without axial loading is calculated to be 3.04 and 7.23 mm, respectively. These estimations are in a good agreement with experimental test results.

Axial strain curves of the steel bars at mid length of the column resulting from strain gauges in the laboratory specimen are drawn in Figure 10 in comparison with FEM results. The strain curves are for front face (up-side) and back face (beneath) of the columns. It was observed that FE analysis can have an appropriate prediction of strain changes during the blast loading. Some discrepancy of the results could occur probably because of unintended noises during the blast event that can affect recorded data.

In the next step of validation of the FE analysis, maximum blast response of the equivalent single-degree-of-freedom (SDOF) system of the considered RC beam (without axial force) was calculated using UFC-3-340-02 [19] methodology (Chapters 3 and 4). For the charge weight of 18 kg-TNT with standoff distance of 3 m, the scaled distance of the blast loading is $Z = 1.14\ \text{m/kg}^{1/3}$. At such scaled distance, one can

Figure 8: Lead rods installed under the specimen.

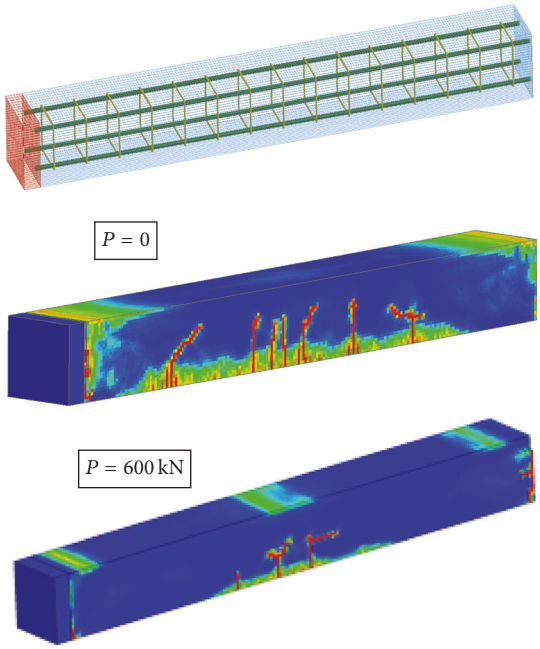

Figure 9: FE modeling and analysis of the columns.

assume uniformly pressure distribution on the structural face [19, 21]. Based on empirical equations proposed by UFC 3-340-02 [19], over-peak pressure (P_{s0} = 0.72 MPa) and positive phase duration (t_0 = 5.1 msec) of the blast wave could be estimated. Dynamic Increase Factor (DIF) for RC members in bending for concrete and reinforcement is 1.05 and 1.17, respectively. Using the methodology introduced in UFC-3-340-02, estimated maximum response of elastoplastic SDOF system under ideal bilinear-triangular pulse is X_m = 9.18 mm. Experimental result of maximum transverse displacement of the specimen without axial load was about 8 mm. It should be noted that generally this method produces a conservative estimate of the blast response of the structure for design purpose [19].

Selected sample for validation axial loading process in FE software is a real column which has been considered as 0C0 in [17] by Hadi and Widiarsa (2012). Geometric characteristics and reinforcing details in this sample are very similar to our own sample. Specifications of this model and its axial test process are shown in Figure 11. Compressive strength of concrete in this sample is equal to 79.5 MPa and yield strength of longitudinal and transverse reinforcement is 564 and 516, respectively [17].

Sample 0C0 is tested under static axial loading and axial load-displacement diagram is drawn for it. Axial load-displacement curves obtained from the experiments are shown in Figure 12(a) [17] in which dashed curve (– – –) is related to 0C0 sample column. Diagrams obtained from FE modeling and experimental testing have been drawn together for better comparison in Figure 12(b). It is evident from Figure 12 that the result of FEM here matches with the experimental results with a good accuracy. Thus, finite element method in this research can be used to continue analysis.

6. Results of Analysis under Blast Loading

Curves in Figure 13 show the results of shear strength-lateral displacement (at the middle height) of the columns. It is evident from Figure 13 that the Col-0 which has not been retrofitted has the lowest shear strength compared to other columns. In this model, the shear strength initially reaches the maximum amount of 300 kN and then slightly increases with slight ups and downs. The initial resistance is greater in other columns compared to Col-0 column. Moreover, the greatest displacement of column's mid height corresponds to unretrofitted column.

Curves in Figure 14 show horizontal displacement history at the columns mid height. For better understanding of the details, results are shown once without Col-0 curve. It is clear that Col-0 has the highest lateral deformation. In addition, the lowest horizontal displacement in the middle height of the columns is observed for Col-3 and Col-4 (maximum amount of about 4 mm). These columns have been strengthened by two steel channels and have shown a high resistance against lateral blast loading. Moreover, Col-5 which is completely covered with steel plates has shown a low deformation (maximum 10 mm). Afterwards, there is Col-2 and Col-1 that

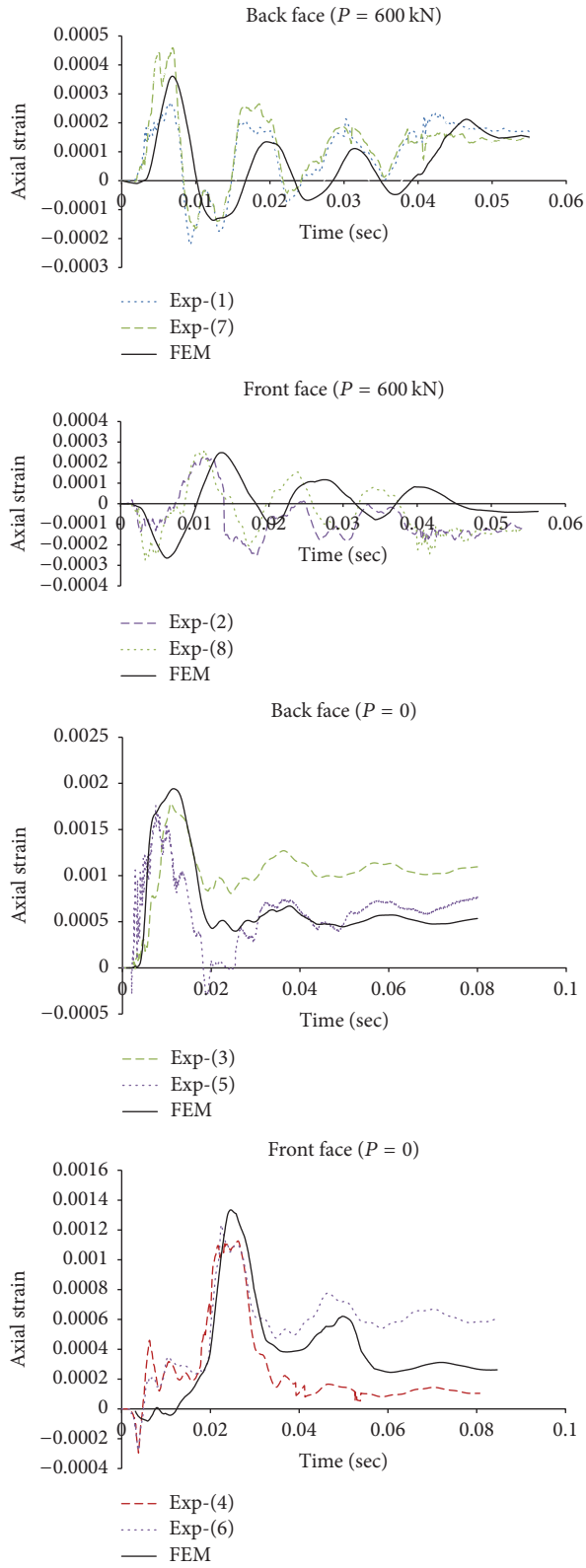

Figure 10: Axial strain-time curves for the longitudinal reinforcement resulting from experimental test and FEM.

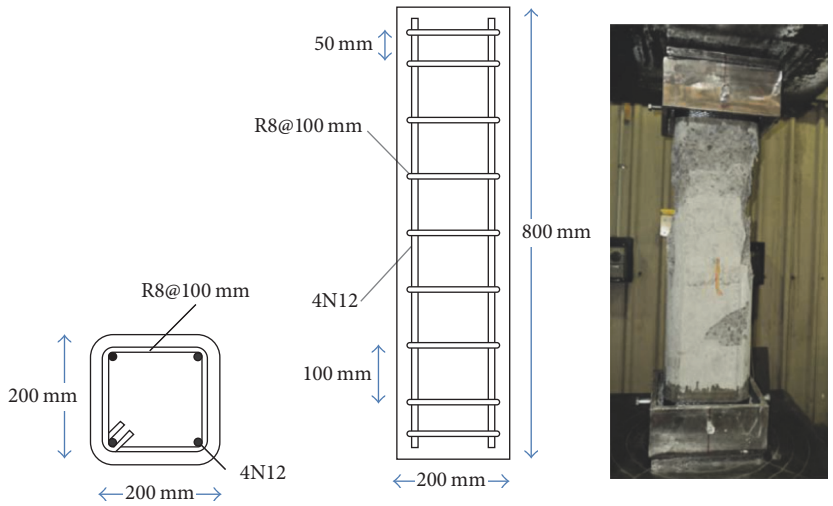

Figure 11: Column sample selected for validation [17].

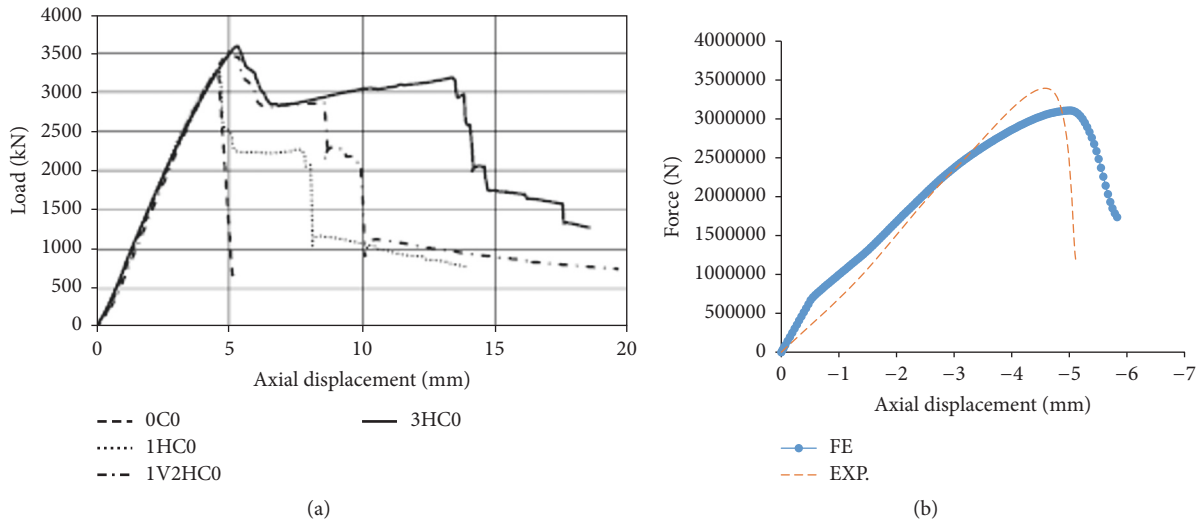

Figure 12: Result of finite element analysis (b) and experimental results [17] (a).

have four steel angles and their maximum displacement is about 16 and 23 mm, respectively.

Based on Figure 14(a), failure mode of RC column without retrofitting (Col-0) is brittle and the column's lateral displacement increases dramatically. However, all strengthened RC columns with steel jackets have more ductile behavior. Belal et al. (2015) demonstrated that specimen strengthened with angles or channel sections (Col-1, 2, 3, and 4) recorded a higher axial strength than that strengthened with plates (Col-5). Moreover, strengthening strategy of Col-4 and Col-1 is more effective than the other methods [16]. Here, we showed that Col-3 and Col-4 have the highest blast capacity than the other columns.

Deformations of reinforcing bars for three column models are shown in Figure 15 for better understanding of the condition of these columns under the effect of blast loading. Figures 15(a) shows the ultimate moments for Col-0 (without retrofitting) under blast loading. Also, Figures 15(b) and 15(c) show the condition of steel bars in Col-3 and Col-5, respectively. It is clear that steel reinforcement in Col-3 does not have considerable deformations and this leads to high resistance of column under the blast loading. On the other hand, there are some plastic deformations in bar grids in Col-5.

Figures 16–21 show the graphical stress contours for 6 columns. Figure 16 shows bending stress in the column without retrofitting (Col-0). Failure conditions can be clearly observed in this figure. In Figures 17–21, bending stress contours (left) and Von-Mises stress in steel jackets (middle) and in the column itself (right) have been shown for 5 retrofitted columns. It is clear that Col-1 (with 3 connecting plates) has a lower resistance and has deformed greater than Col-2 (with 6 connecting plates). Given the fact that columns are fixed at both ends, upper and lower parts of the columns have more critical conditions. Other critical conditions have occurred in connecting plates in

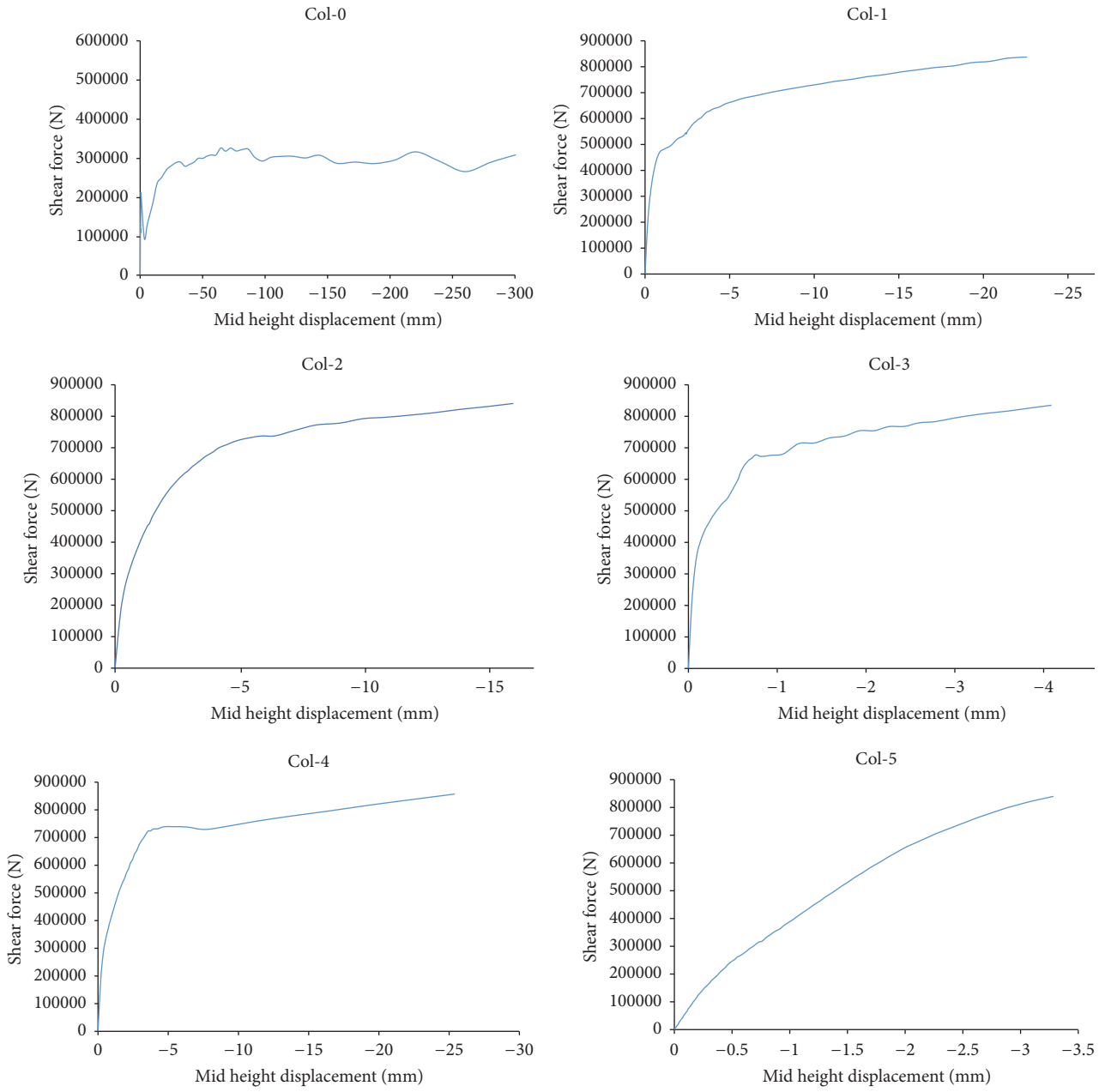

Figure 13: Results of shear strength of columns.

columns with perforated retrofitting. For instance, the middle plate in Col-2 and Col-3 has experienced less von-Mises stress, while other two plates have critical state of stress.

7. Residual Axial Strength

Axial capacity of columns before and after blast loading can define residual axial strength of the column. Residual axial strength is a very important parameter for estimating the overall behavior and progressive collapse of the buildings under the blast loads. Given that residual axial strength is independent of the mode of behavior of the structure, it could be the best criterion for defining damage level of the columns after blast loading [3, 10, 26]. In this paper, after analysis of FE models under lateral blat loading, a compressive uniform axial pressure was applied on one end of the column and failure of the column, ultimate axial load, and its deformation were investigated. In Table 3, P_{u0} axial strength of undamaged RC column (before blast loading) and P_{u1} axial strength of damaged column are summarized. Here, axial strength is assumed to be an axial load level in which by 1% increase in load, displacement increases more than 10%.

According to Table 3, Col-4 and Col-1 undamaged column models have the highest axial capacity. Then, there are Col-2 and Col-3 and the lowest undamaged axial capacity is observed in Col-5 model. After applying blast load, Col-0,

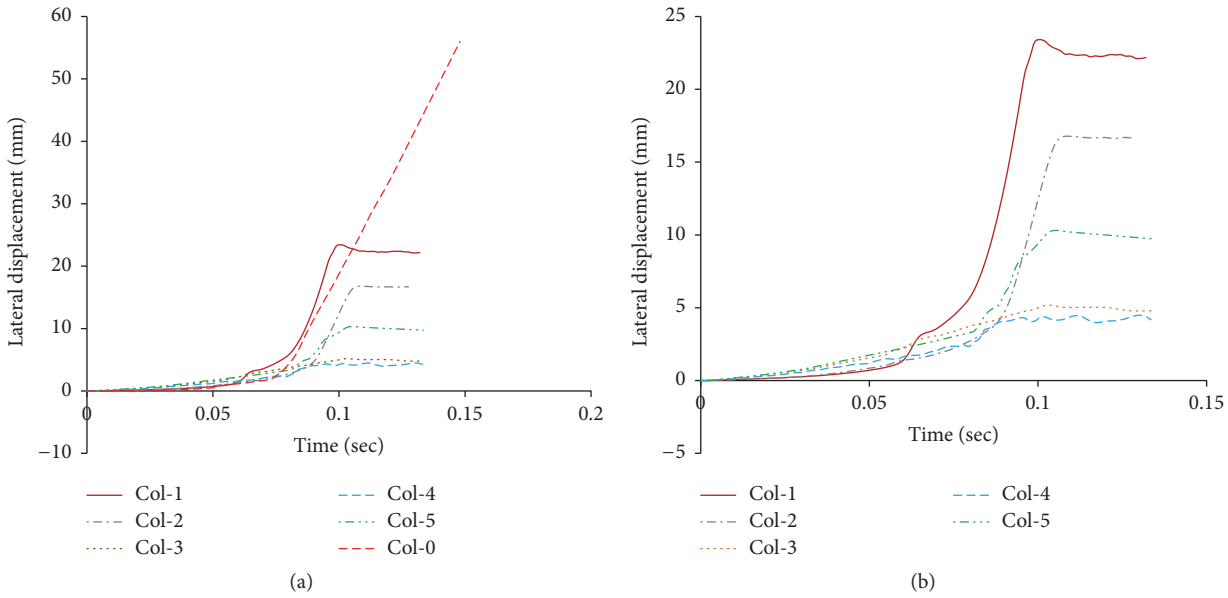

Figure 14: Lateral displacement of column's middle height.

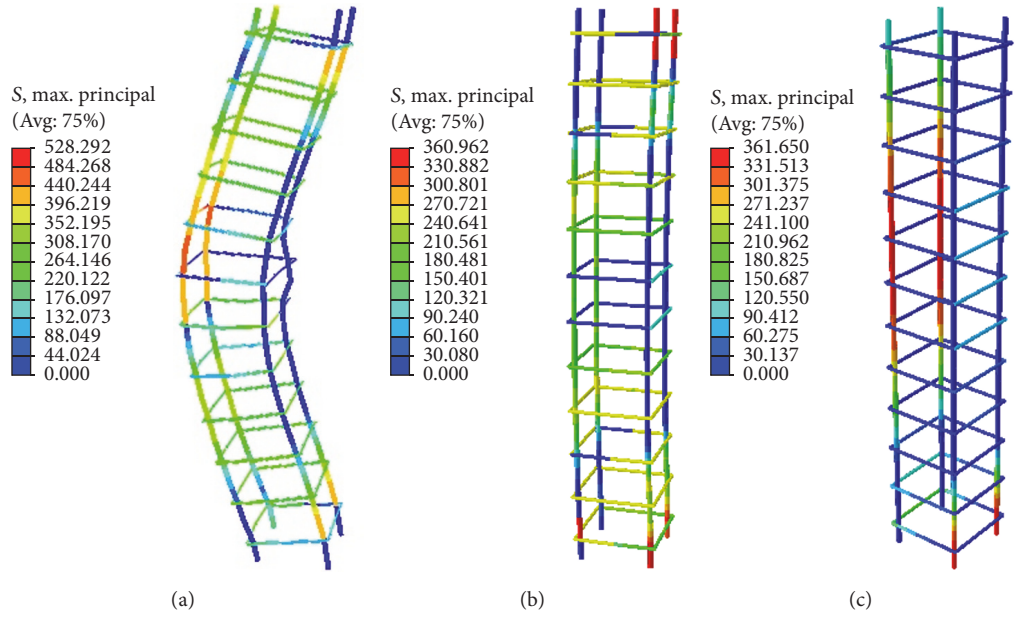

Figure 15: Deformations of steel bars in (a) Col-0, (b) Col-3, and (c) Col-5.

Table 3: Failure loads of the columns.

Model	P_{u0} (kN)	P_{u1} (kN)	P_{u1}/P_{u0}
Col-0	1231	—	—
Col-1	1897	380	0.2
Col-2	1684	791	0.47
Col-3	1627	1506	0.92
Col-4	1873	1762	0.94
Col-5	1524	990	0.65

which is unstrengthened, has lost its whole capacity. The least decrease in axial capacity was observed for Col-4 and Col-3 (6 and 8%, resp.). Axial strength of Col-1 and Col-2 has intensely decreased (80 and 53%, resp.). Buckling of the steel angles could be the reason for this phenomenon.

In Figure 22, deformation shapes of the blast damaged columns under axial load, near the failure state, are shown. According to Figure 22, failure mode in Col-1, 2, 3, 4, and 5 is close to the column's head. However, in Col-0 (without retrofitting), failure occurs through the whole height of the column.

In Figure 23, axial load-displacement curves, after and before blast loading, are drawn. According to Figure 23, residual axial strengths for Col-1 and Col-2 are P_{u1} = 380 and 791 kN and corresponding axial displacements are

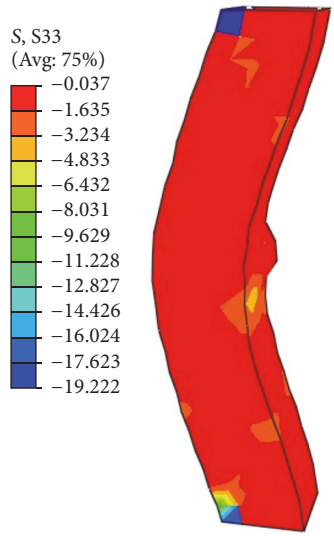

Figure 16: Bending stress in Col-0.

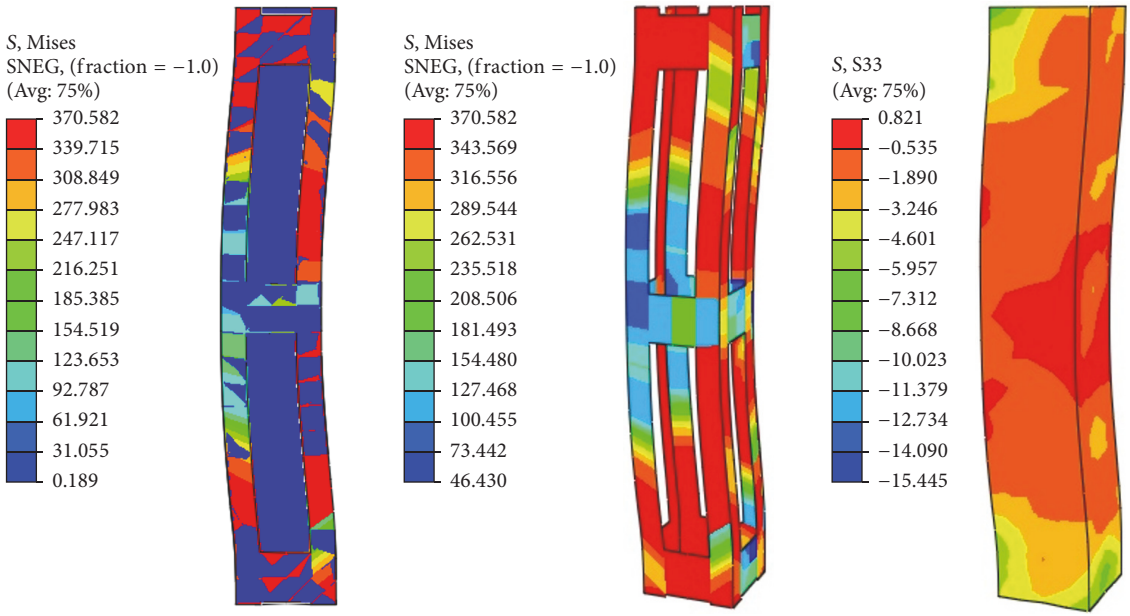

Figure 17: Stress contours in Col-1.

δ_{u1} = 3.2 and 4.79 mm, respectively. It should be noted that deformation of Col-1 is increasing rapidly. In contrast, these values for the undamaged models are P_{u0} = 1897 kN, δ_{u0} = 1.18 mm and P_{u0} = 1684 kN, δ_{u0} = 2.04 mm, respectively. Hence, dramatic decrease in axial capacity and increase in deformation in Col-1 and Col-2 are obvious. In Col-3 and Col-4, which are strengthened by steel channels, maximum axial loads and corresponding deformations, after blast loading, are P_{u1} = 1506 kN, δ_{u1} = 2.01 mm and P_{u1} = 1762 kN, δ_{u1} = 1.27 mm, respectively. For undamaged column models Col-3 and Col-4, maximum axial loads and corresponding deformations are P_{u0} = 1627 kN, δ_{u0} = 1.84 mm and P_{u0} = 1873 kN, δ_{u0} = 1.37 mm, respectively. For Col-5, the difference between the axial capacity and corresponding displacement, before and after blast loading, is more than Col-3 and Col-4 models (P_{u1} = 990 kN, δ_{u1} = 3.65 mm and P_{u0} = 1524 kN, δ_{u0} = 2.11 mm).

8. Conclusion

In this study, the performance of simple and steel jacket strengthened reinforced concrete columns has been evaluated under the effect of blast transverse loading. It should be noted that all of the strengthening configurations originally are used for enhancing the axial capacity of RC columns under pure axial loading. Here, the effectiveness of those strengthening methods on explosion capacity of the RC columns was investigated. Finite element method (FEM) was

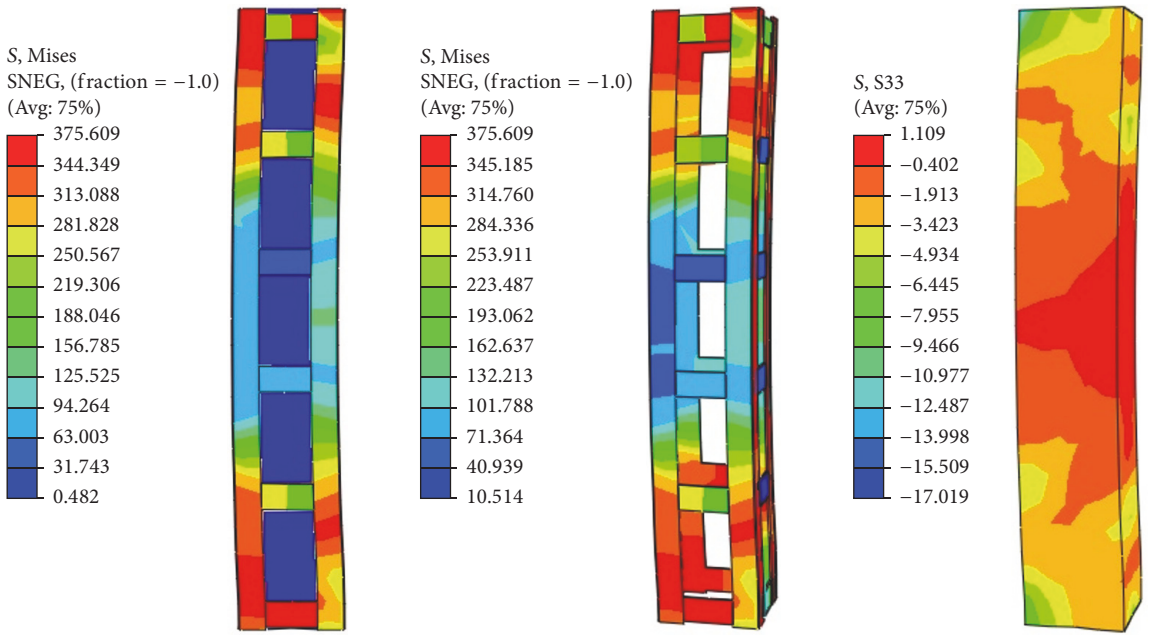

Figure 18: Stress contours in Col-2.

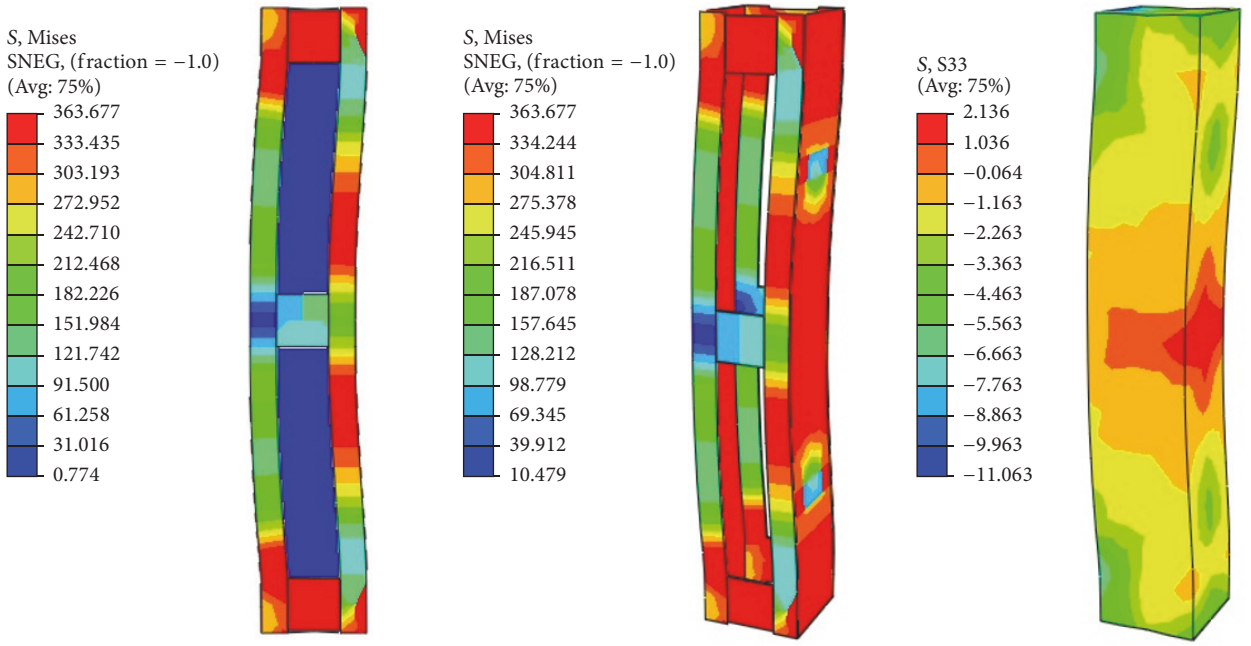

Figure 19: Stress contours in Col-3.

presented for analysis of models using ABAQUS software package. A real scale blast loading test was done by the authors and its results are used for validating FE modeling and analysis process. The test included four RC members with the same geometry and reinforcement details where two samples have initial axial force and two other samples have no axial force. FE modeling of the samples under blast loading showed a good agreement with experimental observations. Afterward, FE modeling process was used for analysis of steel jacket retrofitted columns under lateral blast loading and postblast condition. According to the obtained results, simple column without retrofitting has much less blast resistance compared to retrofitted columns. Thus, retrofitting columns with steel jacket can greatly improve the resistance of columns against explosion loads and extremely enhance residual axial capacity of the RC columns after blast loading.

Retrofitting method with steel channels and connecting plates (Col-4) can be used as an effective way to simultaneously enhance axial and lateral blast resistance of the RC

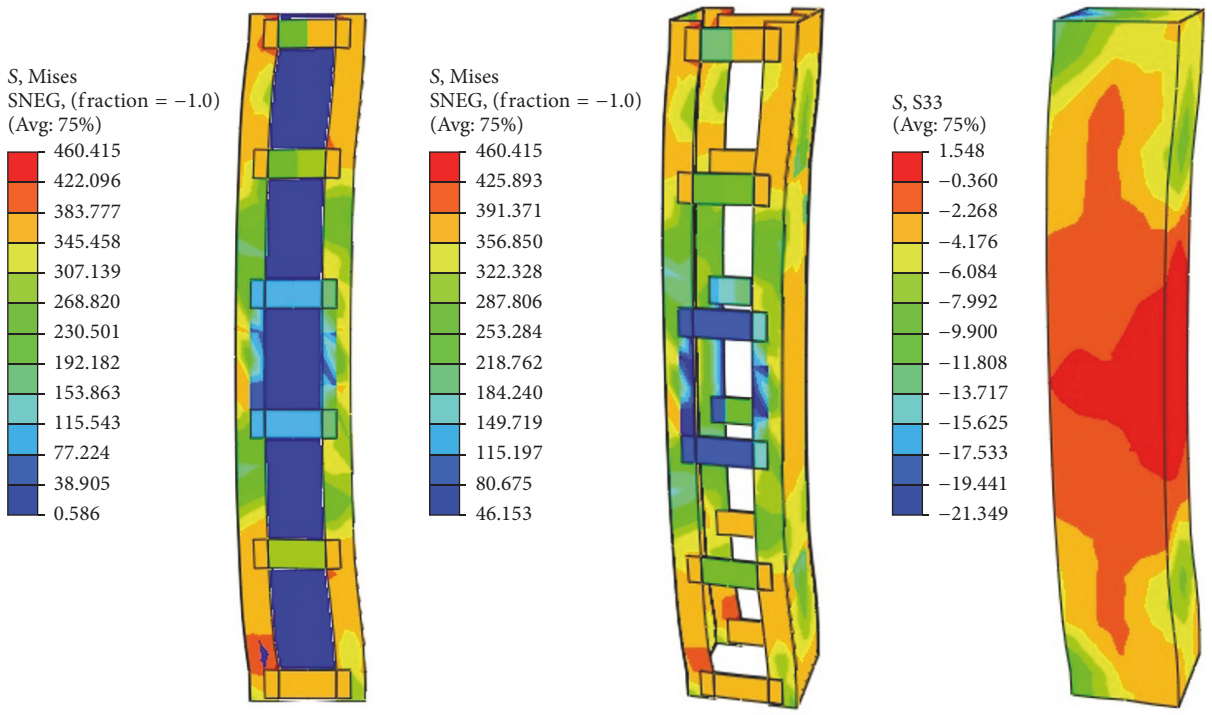

Figure 20: Stress contours in Col-4.

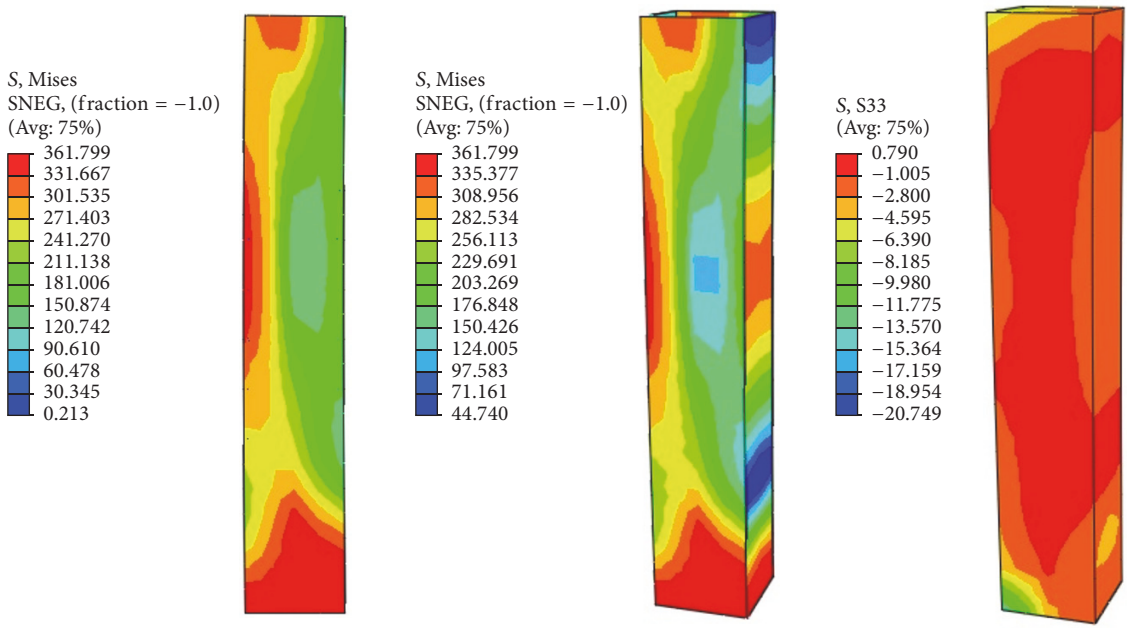

Figure 21: Stress contours in Col-5.

columns. Although strengthening with steel angles (Col-1 and Col-2) has enhancing effects on axial capacity, they are the least effective ways for enhancing blast resistance of the columns. Hence, we can say that deformations of the RC columns under blast loading have the lowest level in retrofitting with steel channel sections compared to steel angles. This fact leads to higher residual strength capacity of the columns strengthened with steel channel sections. However, buckling of the angles under axial load decreases the axial strength of the column. Given the fact that both

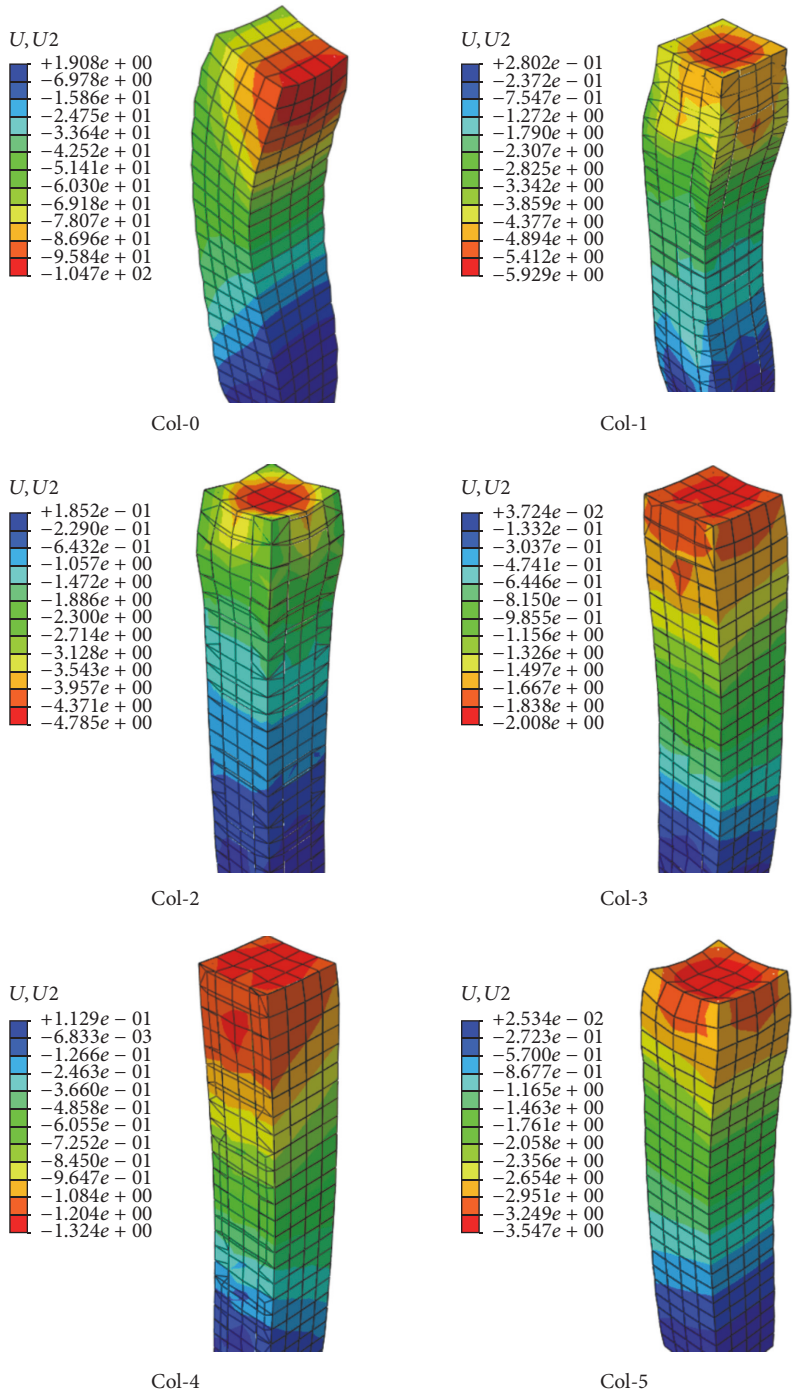

Figure 22: Deformation of damaged columns at failure load.

ends of columns have been assumed to be clamped, the most critical points are located in those areas under blast loading. This critical condition was observed in Col-1 (strengthening with steel angles) and Col-3 (strengthening with steel channels) which have 3 connecting plates in two upper and lower plates.

Generally, it can be said that the results obtained from FEM have been very useful and can have acceptable precision in comparison with experimental test data. Possible differences between finite element analysis results and experimental observations are due to laboratory errors and equipment failure under blast pressure, assumptions of homogeneity of materials, lack of accurate estimation of explosion loads on the structures, and the difference between the actual mechanism of interaction between steel reinforcing bars and concrete. In general, retrofitting with the steel jackets

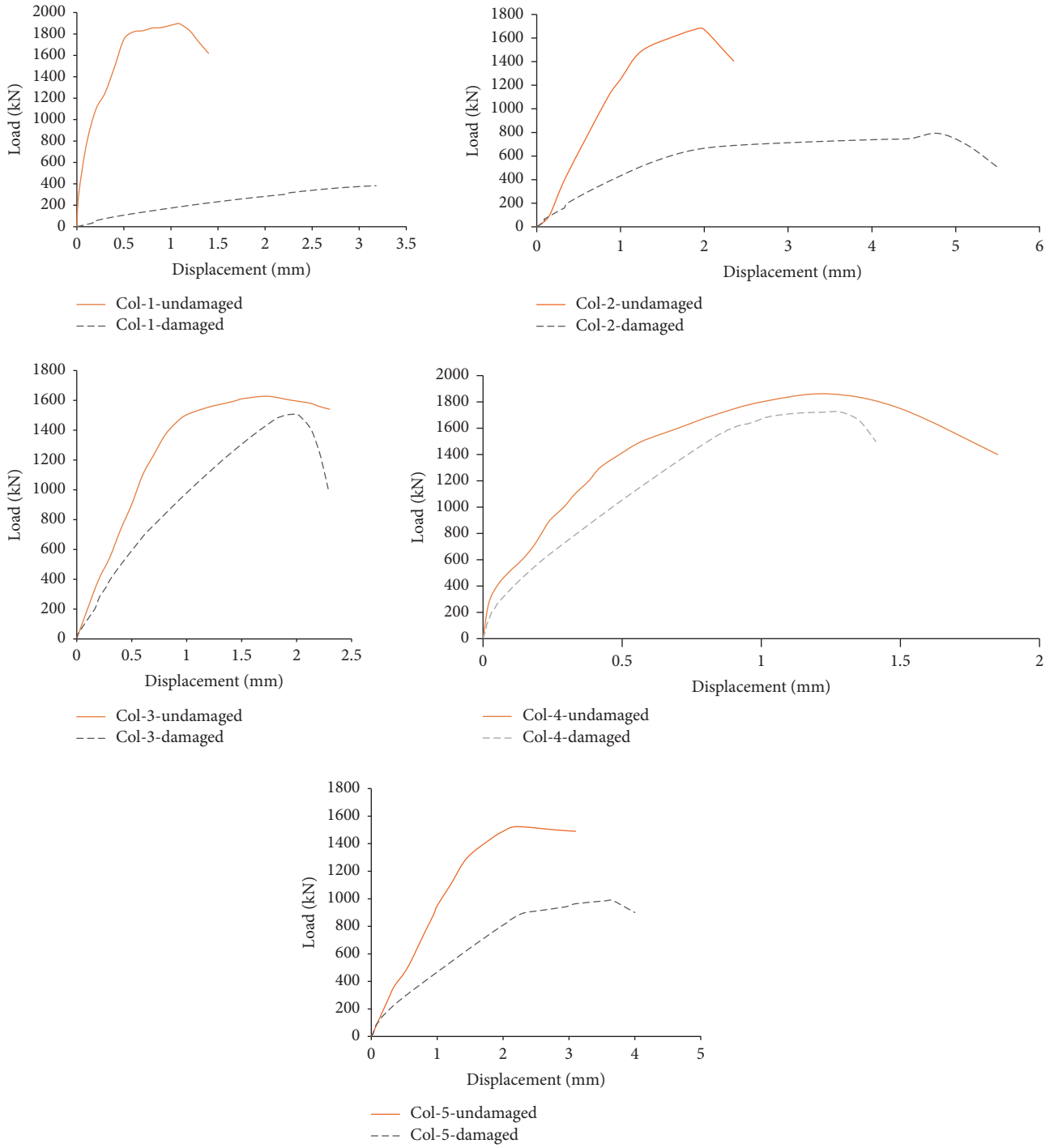

Figure 23: Axial load-displacement curves for the columns before and after blast loading.

would cause a large improvement in the performance of RC columns under the blast loading and their residual axial capacity after blast event.

Conflicts of Interest

The authors declare that there are no conflicts of interest regarding the publication of this paper.

References

[1] P. W. Cooper, *Explosives Engineering*, Wiley-VCH Inc., New York, NY, USA, 1996.

[2] B. Hopkinson, *British Ordnance Minutes; Report No. 13563*, British Ordnance Office, 1915.

[3] X. Bao and B. Li, "Residual strength of blast damaged reinforced concrete columns," *International Journal of Impact Engineering*, vol. 37, no. 3, pp. 295–308, 2010.

[4] T. Rodriguez-Nikl, C.-S. Lee, G. A. Hegemier, and F. Seible, "Experimental performance of concrete columns with composite jackets under blast loading," *Journal of Structural Engineering (United States)*, vol. 138, no. 1, pp. 81–89, 2012.

[5] K. Fujikake and P. Aemlaor, "Damage of reinforced concrete columns under demolition blasting," *Engineering Structures*, vol. 55, pp. 116–125, 2013.

[6] J. E. Crawford, "State of the art for enhancing the blast resistance of reinforced concrete columns with fiber-reinforced plastic," *Canadian Journal of Civil Engineering*, vol. 40, no. 11, pp. 1023–1033, 2013.

[7] J. I. Siddiqui and S. Ahmad, "Impulsive loading on a concrete structure," *Proceedings of the Institution of Civil Engineers: Structures and Buildings*, vol. 160, no. 4, pp. 231–241, 2007.

[8] Y. Shi, H. Hao, and Z. Li, "Numerical derivation of pressure-impulse diagrams for prediction of RC column damage to blast loads," *International Journal of Impact Engineering*, vol. 35, no. 11, pp. 1213–1227, 2008.

[9] K.-C. Wu, B. Li, and K.-C. Tsai, "The effects of explosive mass ratio on residual compressive capacity of contact blast damaged composite columns," *Journal of Constructional Steel Research*, vol. 67, no. 4, pp. 602–612, 2011.

[10] M. Arlery, A. Rouquand, and S. Chhim, "Numerical dynamic simulations for the prediction of damage and loss of capacity of RC column subjected to contact detonations," in *Proceedings of the 8th International Conference on Fracture Mechanics of Concrete and Concrete Structures, FraMCoS 2013*, pp. 1625–1634, Toledo, Spain, March 2013.

[11] C. Kyei and A. Braimah, "Effects of transverse reinforcement spacing on the response of reinforced concrete columns subjected to blast loading," *Engineering Structures*, vol. 142, pp. 148–164, 2017.

[12] M. Carriere, P. J. Heffernan, R. G. Wight, and A. Braimah, "Behaviour of steel reinforced polymer (SRP) strengthened RC members under blast load," *Canadian Journal of Civil Engineering*, vol. 36, no. 8, pp. 1356–1365, 2009.

[13] J. Xu, C. Wu, H. Xiang et al., "Behaviour of ultra high performance fibre reinforced concrete columns subjected to blast loading," *Engineering Structures*, vol. 118, pp. 97–107, 2016.

[14] F. Zhang, C. Wu, X.-L. Zhao, A. Heidarpour, and Z. Li, "Experimental and numerical study of blast resistance of square CFDST columns with steel-fibre reinforced concrete," *Engineering Structures*, 2016.

[15] "Abaqus 6.13 documentation," 2013, https://things.maths.cam.ac.uk/computing/software/abaqus_docs/docs/v6.12/books/usb/default.htm.

[16] M. F. Belal, H. M. Mohamed, and S. A. Morad, "Behavior of reinforced concrete columns strengthened by steel jacket," *HBRC Journal*, vol. 11, no. 2, pp. 201–212, 2015.

[17] M. N. S. Hadi and I. B. R. Widiarsa, "Axial and flexural performance of square RC columns wrapped with CFRP under eccentric loading," *Journal of Composites for Construction*, vol. 16, no. 6, pp. 640–649, 2012.

[18] FEMA (Federal Emergency Management Association), *Designer's Notebook—Blast Consideration*, FEMA Press, 2006.

[19] US Department of Defense (DOD), *tructures to Resist the Effects of Accidental Explosions. UFC 3-340-02*, Wash, USA, 2008.

[20] J. A. Zukas and W. P. Walters, *Explosive Effect and Applications*, Springer, New York, NY, USA, 2002.

[21] "The Design of Structures to Resist the Effects of Accidental Explosions," US Department of Army, Navy and Air Force TM 5-1300, Wash, USA, 1990.

[22] J. Lubliner, J. Oliver, S. Oller, and E. Oñate, "A plastic-damage model for concrete," *International Journal of Solids and Structures*, vol. 25, no. 3, pp. 299–326, 1989.

[23] J. Lee and G. L. Fenves, "Plastic-damage model for cyclic loading of concrete structures," *Journal of Engineering Mechanics*, vol. 124, no. 8, pp. 892–900, 1998.

[24] T. Yu, J. G. Teng, Y. L. Wong, and S. L. Dong, "Finite element modeling of confined concrete-II: Plastic-damage model," *Engineering Structures*, vol. 32, no. 3, pp. 680–691, 2010.

[25] ACI Committee, *Building Code Requirements for Structural Concrete and Commentary (ACI 318-14)*, American Concrete Institute, Farmington Hills, Mich, USA, 2014.

[26] K. Wu, B. Li, and K. Tsai, "Residual axial compression capacity of localized blast-damaged RC columns," *International Journal of Impact Engineering*, vol. 38, no. 1, pp. 29–40, 2011.